Dual-frequency multifunction lidar

Rosemary Diaz*, Sze-Chun Chan, Jia-Ming Liu
Electrical Engineering Department, University of California, Los Angeles,
Los Angeles, CA, USA 90095-1594

ABSTRACT

The design and performance of a continuous wave dual-frequency multifunction lidar system is presented. The system is based on the use of the nonlinear dynamics of an optically injected semiconductor laser. Under proper operating conditions, the laser emits a dual-frequency beam with a broadly tunable microwave separation. The two optical lines are coherently locked to each other using an external microwave synthesizer, resulting in a stable microwave beat frequency. The lidar system is capable of simultaneous velocity and range measurement of remote targets. The velocity is measured from the Doppler shift of the microwave beat frequency. The stability of the microwave beat frequency enables accurate measurement of low velocities. In addition, the stable locking enables long-range measurements because of the long microwave coherence length. Ranging is accomplished by extracting the time-of-flight information carried on the residual microwave phase noise. We demonstrate preliminary measurements of velocities as low as 26 μm/s and range measurements of 7.95 km with 2% accuracy.

Keywords: Laser remote sensing, velocimetry, Doppler lidar, ranging

1. INTRODUCTION

Lidar detection has been widely used since the 1970s. Applications in velocity measurement, imaging, and range finding are widely studied. Early Doppler lidar systems used single-frequency continuous-wave lasers to derive the velocity of a moving target from the frequency shift of the backscattered electromagnetic radiation.[1] Continuous-wave, single-optical-frequency systems are shown to measure velocities down to 5 mm/s over ranges of up to 200 m.[1,2] They are highly sensitive to atmospheric turbulence.

Early laser ranging systems used pulsed laser sources. These systems measure the round-trip time of flight of a laser pulse reflecting off of a distant target. These systems are widely used in various applications. Such systems are limited by electronic noise and errors arising from timing jitter as well as variations in the laser pulse amplitude and shape.

Lidar techniques have evolved to enable the use of various laser sources to accomplish different tasks. For example, a method known as dual-frequency Doppler- lidar (DFDL) enables the measurement of the velocity of a moving target.[3] This method utilizes a microwave beat frequency that results from two different optical frequencies. This has been done in a couple of ways, either by externally modulating the laser[4] or overlapping two laser beams with a known frequency difference.[3] However, these techniques require careful alignment, and operate within a limited microwave frequency range (up to 3 GHz). Systems are bulky, difficult to maintain, and expensive. On the other hand, new developments in laser ranging[5] include frequency modulation of a continuous wave laser diode where the current is ramped up and down externally to effectively sweep the optical frequency. Half of the beam is sent to a reference detector, while the other half of the beam probes a distant target. The round-trip time of flight of the target beam is determined by combining the two beams and measuring the instantaneous frequency difference. Limitations of this include nonlinearity of the response, and the optical coherence length of the laser diode. Each system has its unique advantages and limitations, and is usually designed to accomplish one specific task.

In this paper we present a dual-frequency multifunction lidar system that utilizes a tunable, coherently locked, dual-frequency laser source to measure both velocities and range accurately. When it functions as a DFDL system, it measures velocities as low as 26 μm/s. The dual-frequency source is generated by exploiting the nonlinear dynamics of semiconductor lasers.[6,7] There is much research in the area of nonlinear dynamics of optically injected semiconductor lasers.[8-11] The source used here has an optical injection configuration where a master laser optically injects a slave laser. Recent work has shown that this system can be used as a laser range-finder as well. Preliminary results are presented.

*rdiaz@ee.ucla.edu

Free-Space Laser Communication Technologies XIX and Atmospheric
Propagation of Electromagnetic Waves, edited by Steve Mecherle, Olga Korotkova,
Proc. of SPIE Vol. 6457, 64570O, (2007) · 0277-786X/07/$18 · doi: 10.1117/12.699822

2. METHODOLOGY

A schematic of the experimental setup is shown in Fig. 1. In this experiment, we use single-mode distributed feedback semiconductor lasers operating at 1.3 μm. It is important to note that this technique can also be applied to semiconductor lasers operating at eye-safe wavelengths. The lasers are independently controlled and are temperature and current stabilized. The master laser (ML) is detuned 2.3 GHz from the free-running frequency of the slave laser (SL). The half-wave plates (HW) and the Faraday rotator (FR) are arranged such that the master laser injects the slave laser while the output of the slave laser is completely transmitted through the first polarizing beam splitter (PBS1). The injection strength is adjusted with a variable attenuator (VA). Under proper operating conditions, the optical injection drives the slave laser into the period-one dynamic state, where it emits a dual-frequency beam.[11] The two components have nearly equal amplitudes and are separated by a broadly tunable (10–100 GHz) microwave frequency. When the system operates in the period-one state, the resulting beat frequency has a microwave linewidth of about 10 MHz. However, it is easily and significantly reduced by injecting the slave laser with a weak microwave modulation (at the period-one frequency) from a microwave frequency synthesizer (MFS) using the double-lock technique demonstrated by Simpson and Doft.[6] This locks the two optical lines in phase with each other. As a result, the linewidth of the detected microwave beat frequency is narrow (less than 1 kHz) resulting in a long microwave coherence length. A detailed study of the optical and microwave spectra of the period-one dynamic state is documented in Ref. 7.

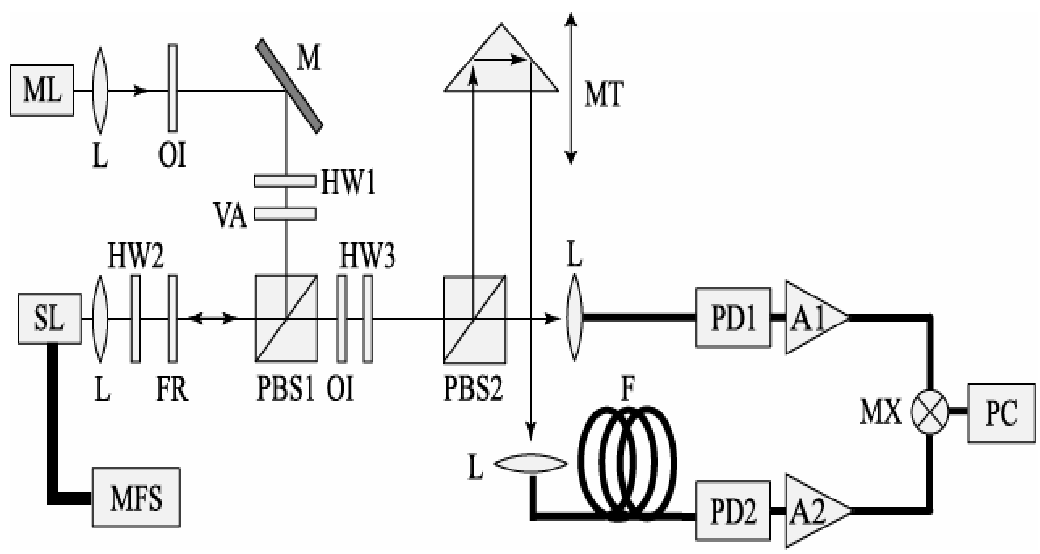

Fig. 1. Schematic of the experimental setup. ML: master laser; SL: slave laser; OI: optical isolator; HW: half-wave plate; VA: variable attenuator; FR: Faraday rotator; PBS: polarizing beam splitter; L: lens; M: mirror; MT: moving target; F: fiber spool; PD: high-speed photodiode; A: microwave amplifier; MX: microwave mixer; PC: computer; MFS: microwave frequency synthesizer.

The second polarizing beam splitter (PBS2) spits the light into two parts. The transmitted part of the beam is directly detected by high-speed photodiode PD1, which is referred to as the reference photodiode. The reflected part of the beam is directed to a moving target (MT). The target is an uncoated right-angle prism mounted on a translation stage that is driven at a nearly constant velocity by a motorized actuator. By total internal reflection inside the prism, the beam is reflected back toward a second high-speed photodiode PD2, referred to as the target photodiode. When the target is in motion, the detected signal at PD2 is Doppler shifted. The Doppler shift is extracted by mixing the signals of PD1 and PD2 by using a microwave mixer (MX). The output of the mixer is sent to a data acquisition system and is recorded on a computer. A 5.5 km length of fiber (approximately 8 km optical path) is between the collection lens and PD2 to demonstrate the long-range ability of this system.

The dual-frequency optical electric field of the slave laser with frequencies ν_1 and ν_2 and amplitudes E_1 and E_2 received by the reference photodetector is

$$E_r = \left\{E_1 e^{i\phi_1(t)} + E_2 e^{i(\phi_2(t)-2\pi f_{RF} t)}\right\} e^{-i2\pi\nu_1 t} \tag{1}$$

where $f_{RF}=\nu_2-\nu_1$ is the microwave frequency difference and $\phi_1(t)$ and $\phi_2(t)$ are the random phase noise terms responsible for the optical linewidths of ν_1 and ν_2, respectively. Upon photodetection, this phase noise contributes to the linewidth of the microwave frequency. The signal received by the target photodiode experiences a delay during its round trip to the target. The optical electric field in the target arm is

$$E_t = \left\{E_1 e^{i\phi_1(t-\tau)} + E_2 e^{i(\phi_2(t-\tau)+2Kx-2\pi f_{RF} t)}\right\} e^{-i2\pi\nu_1(t-\tau)} \tag{2}$$

where x is the position of the target, c is the speed of light, $\tau=2x/c$ is the round-trip delay time, and $K=2\pi f_{RF}/c$ is the effective microwave propagation constant. The detected current signals from the reference and target photodiodes, respectively, are

$$I_r = 2G_r E_1 E_2 \cos(2\pi f_{RF} t - \Delta\phi(t)) \tag{3}$$

$$I_t = 2G_t E_1 E_2 \cos(2\pi f_{RF} t - 2Kx - \Delta\phi(t-\tau)) \tag{4}$$

where $\Delta\phi(t)=\phi_2(t)-\phi_1(t)$ and G_r and G_t are the amplifier gains for the reference and target beams, respectively. These two current signals are sent to an RF mixer giving a signal proportional to the product of $I_r(t)$ and $I_t(t)$:

$$P_{mix} = 2A\cos(2Kx(t) - \Phi) \tag{5}$$

with $A=G_rG_tE_1E_2$ and $\Phi=\Delta\phi(t)-\Delta\phi(t-\tau)$. In the following subsections, we will consider targets moving at a constant velocity, targets moving sinusoidally, and targets moving periodically back and forth at a constant velocity.

2.1 Targets moving at a constant velocity

When the laser beam is directed to a target that moves at a constant velocity v, $x(t)=d+vt$, where d is the initial distance of the target. We have

$$P_{mix} = 2A\cos(2\pi f_{RF}^{D} t + 4\pi d f_{RF}/c - \Phi), \tag{6}$$

where $f_{RF}^{D}=2vf_{RF}/c$ is the Doppler-shift frequency. The Doppler shift f_{RF}^{D} is obtained by taking the power spectral density (PSD) of P_{mix}. Thus, the magnitude of the velocity is measured. While it is not the intent of this paper to determine the direction of motion, it can be easily determined by implementing an in-phase and quadrature detection as demonstrated by Morvan *et al*.[4]

2.2 Sinusoidal Motion

Targets moving sinusoidally with amplitude x_0 and oscillation frequency f_{osc} can be described as

$$x(t) = x_0 \sin(2\pi f_{osc} t). \tag{7}$$

Substituting this in Equation 5, the detected signal is

$$P_{mix} = 2A\cos\left(\frac{4\pi x_0}{\Lambda}\sin 2\pi f_{osc} t - \Phi\right) \tag{8}$$

where $\Lambda=2\pi/K$ is the microwave wavelength. The peak velocity is $v_p=2\pi x_0 f_{osc}$, and the peak Doppler shift is $f_{RF}^{D}=4\pi x_0 f_{osc} f_{RF}/c$. The oscillation frequency of the target is therefore $f_{osc}=c\, f_{RF}^{D}/4\pi x_0 f_{RF}$. Substituting this in Equation 8, the mixer output becomes

$$P_{\mathrm{mix}} = 2A\cos\left(\frac{4\pi x_0}{\Lambda}\sin\frac{f_{RF}^{D}\Lambda}{4\pi x_0}t - \Phi\right). \tag{9}$$

Using this result, we simulate signals that would result at the output of the mixer and calculate the corresponding PSD. It is important to understand the limitation that results from using a microwave frequency for measurement. That is, in order to correctly calculate the Doppler shift frequency, either the target must move with a sufficiently large amplitude, x_0, or the microwave wavelength must be sufficiently short. We examine four cases in the following simulated data: x_0/Λ=0.1,1,10, and 100. Letting the Doppler shift stay fixed at 1 Hz with an arbitrary phase shift $\Phi=\pi/4$, we examine the mixer output signal and the corresponding power spectra.

Examining Figs. 2(a) and (b), it is clear that the measured Doppler shift frequency is incorrect when the ratio between the displacement amplitude and the microwave wavelength is 0.1. Specifically, the oscillation frequency, rather than the Doppler shift frequency, is measured. In this case, x_0 is small compared with the RF wavelength. As a consequence, the target continues to change direction before a full period of the Doppler shift frequency signal is acquired. Examining figures 2(c) and (d), we see that the Doppler shift peak is incorrect because once again, the ratio $x_0/\Lambda=1$ is too small, and we are once again unable to acquire several periods of the Doppler shift frequency signal. Figure 2(e) shows complete cycles of the Doppler frequency; however, Fig. 2(f) shows that the Doppler frequency is somewhat masked by sidebands of the oscillation frequency. Finally in Figs. 2(g) and (h), we see that the peak Doppler shift is clearly 1 Hz. Hence, when measuring the velocity of a target that moves sinusoidally, it is important to measure a target that has a displacement amplitude at least 100 times the RF wavelength.

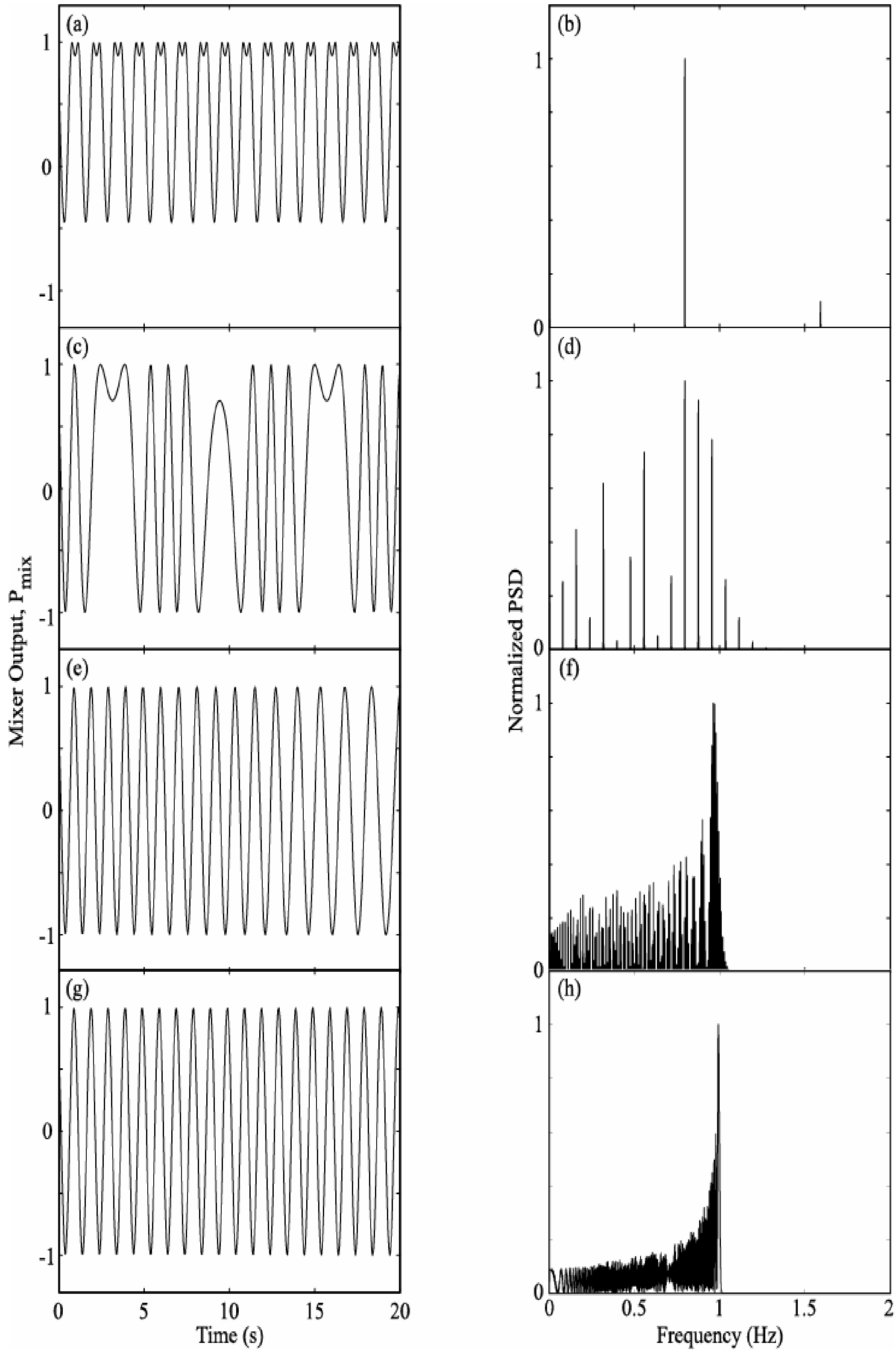

Figure 2. Simulation results of the mixer output and corresponding PSD for a target that moves sinusoidally. The expected Doppler shift frequency is 1 Hz. We examine the signals when the ratio x_0/Λ is: (a) and (b) 0.1, (c) and (d) 1, (e) and (f) 10, and (g) and (h) 100.

2.3 Periodic Motion

Consider a target moving back and forth as a triangular wave with amplitude x_0 and oscillation frequency f_{osc}. We can describe this motion as

$$x(t) = \frac{8x_0}{\pi^2} \sum_{n=0}^{\infty} \frac{1}{(2n+1)^2} \cos[(2n+1)2\pi f_{\text{osc}} t]. \tag{10}$$

Substituting this in Equation 5 yields

$$P_{\text{mix}} = 2A\cos\left(\frac{32x_0}{\pi\Lambda} \sum_{n=0}^{\infty} \frac{1}{(2n+1)^2} \cos[(2n+1)2\pi f_{\text{osc}} t] - \Phi \right). \tag{11}$$

The target has a peak velocity $v_p=4x_0 f_{\text{osc}}$ and a peak Doppler shift $f_{\text{RF}}^{\text{D}}=8x_0 f_{\text{osc}}/\Lambda$. The oscillation frequency of the target is therefore $f_{\text{osc}}=\Lambda f_{\text{RF}}^{\text{D}}/8x_o$. Substituting this in Equation 11, the mixer output becomes

$$P_{\text{mix}} = 2A\cos\left(\frac{32x_0}{\pi\Lambda} \sum_{n=0}^{\infty} \frac{1}{(2n+1)^2} \cos\left[(2n+1) \frac{2\pi\Lambda f_{\text{RF}}^{\text{D}}}{8x_0} t \right] - \Phi \right). \tag{12}$$

Using this result, we simulate signals that would result at the output of the mixer and calculate the corresponding PSD. Letting the Doppler shift =1 Hz, and $\Phi=\pi/4$, we once again examine the measured frequency in four different cases: x_0/Λ=0.1,1,10, and 100. Figure 3 shows the mixer output and corresponding PSD for all four cases. Figures 3(a) and (b) show that the oscillation frequency is measured rather than the Doppler shift frequency. This is a direct consequence of not acquiring full cycles of the microwave frequency. Figures 2(c) and (d) show the correct Doppler shift peak surrounded by sidebands of the oscillation frequency. Thus the ratio $x_0/\Lambda=1$ for a target that moves periodically back and forth at a constant velocity enables one to acquire several periods of the Doppler shift frequency signal. Figures 2(e) –(h) show the signals are increasingly clear as the ratio between x_0 and Λ increase, resulting in a clear 1 Hz Doppler frequency.

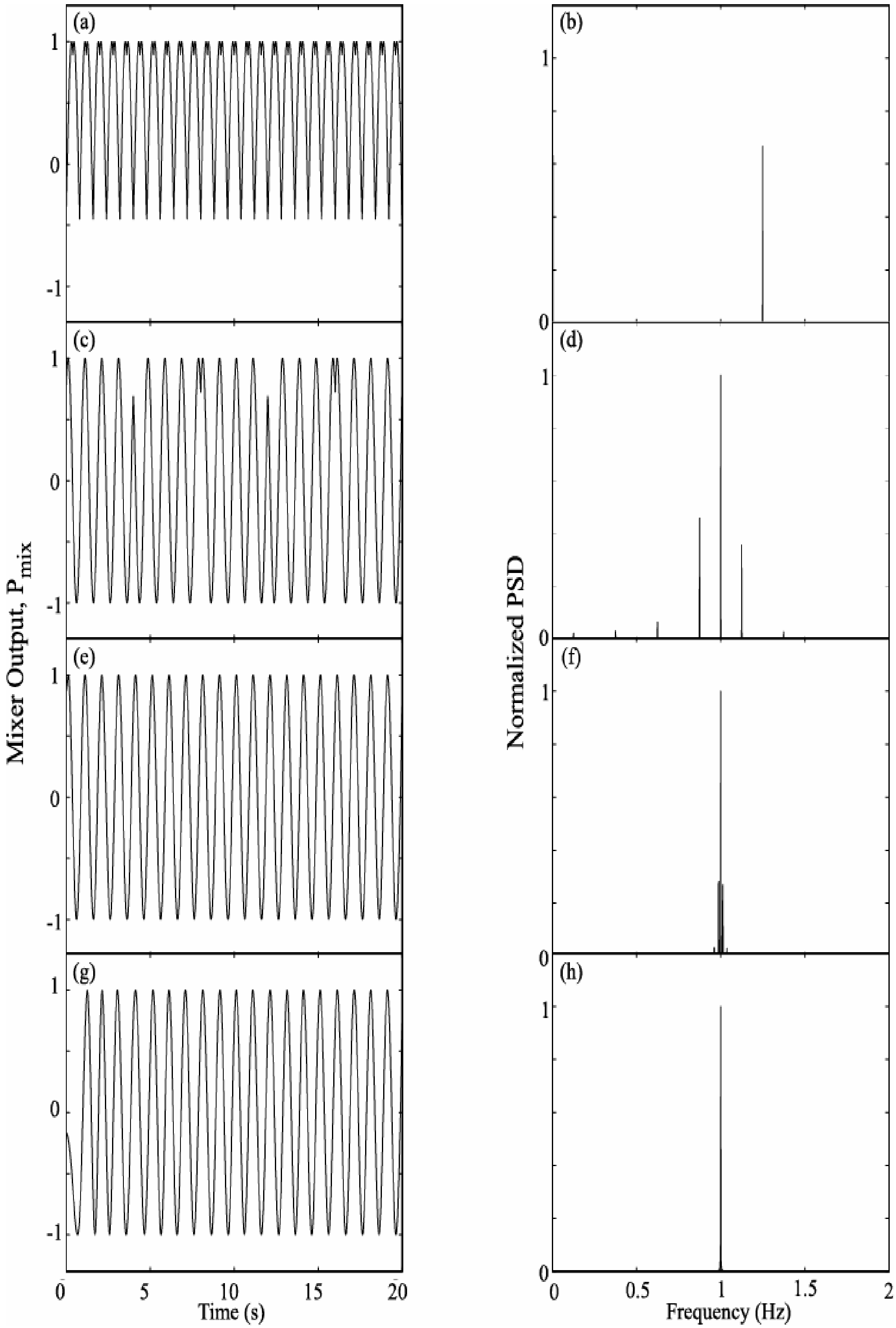

Figure 3. Simulation results of the mixer output and corresponding PSD for a target that moves periodically at a constant velocity. The expected Doppler shift frequency is 1 Hz. We examine the signals when the ratio x_0/Λ is: (a) and (b) 0.1, (c) and (d) 1, (e) and (f) 10, and (g) and (h) 100.

3. DATA

3.1 Doppler lidar

As shown in Equation 6, the microwave Doppler shift is measured rather than the optical Doppler shift. Thus, velocity information is obtained from the Doppler-shifted microwave signal. Doppler measurements depend on only the optical frequency difference, not on the optical frequencies themselves. Accurate velocity measurement thus depends on the microwave stability rather than the optical frequency stability. Note that the optical linewidth does not affect the performance of the system. As mentioned in Section 2, the period-one oscillation results in a microwave beat signal with a microwave linewidth of 10 MHz.[7] This limits the range of measurement to approximately 2.4 m. Adding the external modulation to the slave laser significantly improves the range limit to more than 24 km, as the microwave linewidth is less than 1 kHz resulting in a long microwave coherence length.

Experiments were carried out to demonstrate the performance of the DFDL. The data obtained from an experiment with f_{RF}=17 GHz is shown below. This system is capable of generating frequencies of up to 100 GHz.[10-11] However, due to electronic bandwidth limitations, the period-one oscillation frequency was kept below 20 GHz in the experiment reported here. In this experiment 1000 s of data were collected in order to achieve millihertz resolution. Figure 4 shows the normalized PSD of the mixer output data shown in the inset. The measured Doppler-shift frequency of f_{RF}^{D}=3 mHz yields a velocity of 26 μm/s, which is in excellent agreement with an independent measurement of the target velocity that also yielded 26 μm/s. The system was used to accurately measure a wide range of velocities over various distances. The results are reported in Ref. 12.

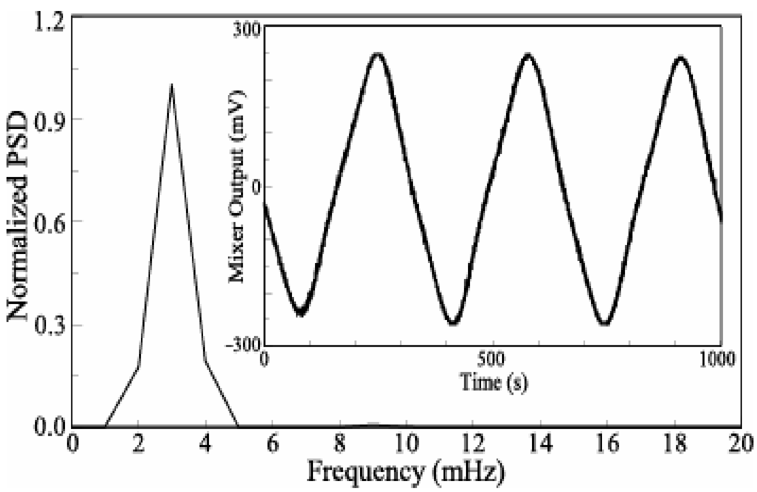

Fig. 4 The inset figure shows the mixer output for f_{RF}=17 GHz. The target moves away from the detector at 26 μm/s. The main figure shows the normalized PSD where the Doppler shift is 3 mHz.

3.2 Ranging

Recent work shows that the system is capable of measuring the range to a target. The same experimental setup shown in Fig. 1 is used for the ranging demonstration with two slight modifications: 1) rather than sending the output of the mixer to a computer, we send it to a power spectrum analyzer and 2) the target is stationary. Recall that the target arm contains a fiber spool that is approximately 8 km of optical path. When looking at a frequency span from 0-2 MHz, a periodic feature is present in the power spectrum as shown in Fig. 5. The period of the power spectrum contains time of flight information. The preliminary measurement shown here demonstrates the potential of the system as a ranging lidar. The adjacent peaks in the power spectrum are measured to be 37.74 kHz, the reciprocal of the time of flight. This corresponds to an optical path difference between the reference and target arms of 7.95 km.

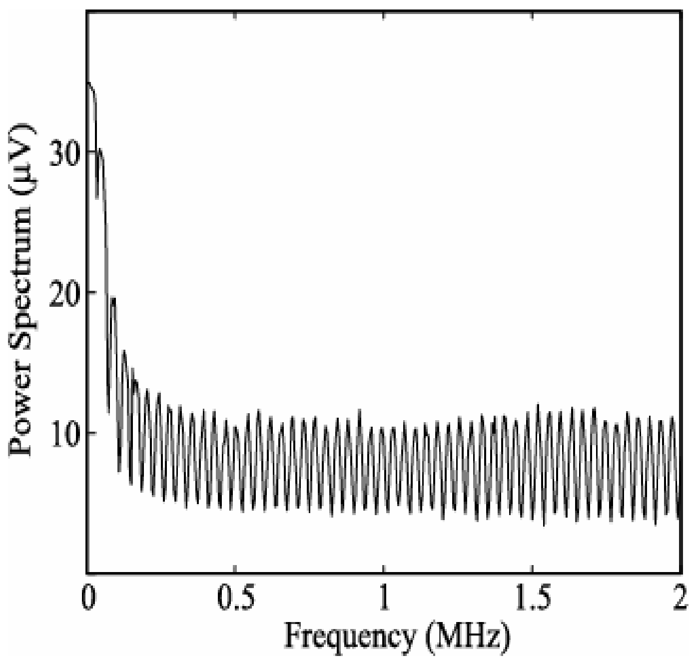

Figure 5. The power spectrum of the mixer output is measured. The frequency of the periodic structure is calculated by taking the Fourier transform of this data. The spacing between adjacent peaks is calculated to be 37.74 kHz, which corresponds to an optical path difference between the reference and the target arm of 7.95 km.

4. CONCLUSION

We have demonstrated the use of a coherently locked dual-frequency beam that is generated by using nonlinear laser dynamics for Doppler-lidar detection. The two optical frequencies are separated by a tunable microwave frequency and are locked by an external microwave modulation, resulting in an intensity that oscillates at the beat frequency. When the beam is incident on a moving target, both optical frequencies experience a Doppler shift, resulting in a shifted beat frequency. The shift of the beat frequency is extracted by electrically mixing with the original signal, hence yielding the velocity. Due to the stability of the microwave and the elimination of common noise, accurate velocity measurement is possible. Experiments of velocity measurement are carried out to demonstrate the feasibility of the DFDL. Using a coherently locked dual-frequency beam with the frequencies separated by 17 GHz, we are able to accurately measure velocity as low as 26 μm/s over long ranges. We also demonstrated the system's ability for ranging. Future work will involve optical amplification of the dual-frequency beam for field-testing. With the advantages of compact size, low cost, and light-weight, DFDL has great potential in applications such as remote and portable detection.

REFERENCES

1. R. T. Menzies and R. M. Hardesty, "Coherent Doppler lidar for measurements of wind fields," Proc. IEEE 77(3),449-462 (1989)
2. H. W. Mocker and P. E. Bjork, "High accuracy laser Doppler velocimeter using stable long-wavelength semiconductor lasers," Appl. Opt. 28(22), 4914-4919 (1989).
3. W. L Eberhard and R. M. Schotland, "Dual-frequency Doppler-lidar method of wind measurement," Appl. Opt., 19(17), 2967-2976 (1980)
4. L. Morvan, N. D. Lai, D. Dolfi, J. P. Huignard, M. Brunel, F. Bretenaker, and A. LeFloch, "Building blocks for a two-frequency laser lidar-radar: a preliminary study," Appl. Opt., 41(27), 5702-5712 (2002)
5. M. C. Amann, T. Bosch, M. Lescure, R. Myllylä, M. Rioux, "Laser ranging: a critical review of usual techniques for distance measurement," Opt. Eng. 40(1), 10-19 (2001)

6. T. B. Simpson and F. Doft, “Double-locked laser diode for microwave photonics applications,” IEEE Photon. Technol. Lett. 11(11), 1476-1478 (1999)
7. S. C. Chan and J. M. Liu, “Tunable narrow-linewidth photonic microwave generation using semiconductor laser dynamics,” IEEE J. Sel. Top. Quantum Electron., 10(5), 1025-1032 (2004)
8. S. K. Hwang and J. M. Liu, “Dynamical characteristics of an optically injected semiconductor laser,” Opt. Commun., 183, 195-205 (2000)
9. T. B. Simpson, J. M. Liu, K. F. Huang, and K. Tai, “Nonlinear dynamics induced by external optical injection in semiconductor lasers,” Quantum Semiclassic. Opt. 9, 765-784 (1997)
10. S. K. Hwang, J. M. Liu, and J. K. White, “Characteristics of period-one oscillations in semiconductor lasers subject to optical injection,” IEEE J. Sel. Top. Quantum Electron., 10(5), 974-981 (2004)
11. S. C. Chan and J. M. Liu, “Frequency Modulation on single sideband using controlled dynamics of an optically injected semiconductor laser,” IEEE J. Quantum Electron., 42(7), 699-705 (2006)
12. R. Diaz, S. C. Chan and J. M. Liu, “Lidar detection using a dual-frequency source,” Opt. Lett., 31(24), 3600-3602 (2006)